Development of Poly(vinylidene fluoride) Hollow-Fiber Membranes for the Treatment of Water/Organic Vapor Mixtures

S. CHABOT,[1] C. ROY,[1] G. CHOWDHURY,[2] T. MATSUURA[2]

[1] Department of Chemical Engineering, Université Laval, Sainte-Foy, Québec G1K 7P4, Canada

[2] Department of Chemical Engineering, University of Ottawa, Ottawa, Ontario K1N 6N5, Canada

Received 5 July 1996; accepted 5 January 1997

ABSTRACT: Attempts were made to spin hollow-fiber membranes from poly(vinylidene fluoride) (PVDF) material by the dry–wet phase inversion method. Hollow fibers so prepared were characterized for various parameters and by electron microscopic techniques. Membranes were also tested for the separation of water/1-propanol mixtures in vapor phase. It was found that the hollow fibers were water selective despite the fact that PVDF material is hydrophobic. Intrinsically organic selective property of PVDF material was proved by coating a porous polyetherimide membrane with a PVDF layer, which resulted in enhancement of 1-propanol permeation while suppressing the permeation of water. © 1997 John Wiley & Sons, Inc. J Appl Polym Sci **65:** 1263–1270, 1997

Key words: PVDF; hollow-fiber membrane; vacuum pyrolysis; vapor permeation

INTRODUCTION

Today every new process has to be under the strict control of environmental regulations. The removal of organic wastes is, therefore, becoming increasingly important, and vacuum pyrolysis finds its application in this area. The latter process presents advantages over other conventional processes. Organic material is usually transformed to oils, solids, and gas, in that order. Gas can be burned to provide energy to the system. Oils also can be burned or better, be upgraded to enhance the value of some components. Pyrolytic water is also produced when oxygenated materials are treated. When vacuum pyrolysis is applied to a feedstock containing water such as contaminated soils, urban wastes, and biomass, a large quantity of water needs to be treated before being drained to the sewer.[1–3]

There are many processes for the treatment of water. Decantation may be the least expensive among those processes. Decantation is, however, applicable only when at least two liquid phases are present.[4] Aqueous solutions formed by pyrolytic processes are often composed of only one phase, where water is saturated with organic compounds. Decantation is, therefore, impossible.

Biological process for water treatment is commonly used and relatively inexpensive. Biological treatment, however, requires a large space. It also requires a stable aqueous phase where bacteria can be accumulated to decompose the organic material. This restricts the use of this process for the treatment of pyrolytic aqueous product, as the composition of the pyrolytic product may vary rapidly with a change in feedstock. For example, soil contaminated with hydrocarbons may change to soil contaminated with PCB within a short period. Bacteria cannot adjust themselves rapidly enough to decompose PCB. They may even die in a new environment.[5]

Other processes such as catalytic oxidation[6,7]

Correspondence to: C. Roy.

 CCC 0021-8995/97/071263-08

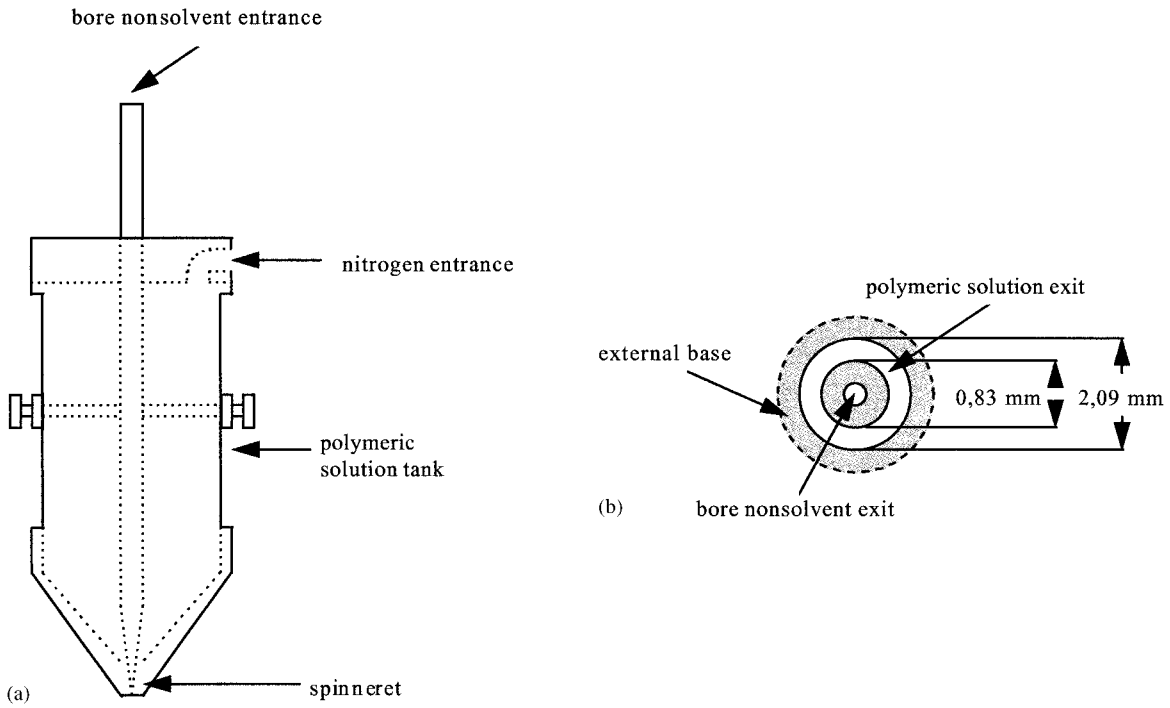

Figure 1 Design of spinneret: (a) global view; (b) simple nonsolvent exit spinneret.

and adsorption on activated carbon[8–10] are often too expensive for industrial applications.

An alternative that is also novel, inexpensive, and flexible is the membrane process. Membrane separation in the vapor phase is very attractive, particularly when steam and organics already exist in the vapor phase. The membrane process is self-adjusting to a change of the feed. Moreover, the flux of vapor permeation is higher than that of pervaporation, which is another membrane process preferably used when the aqueous feed mixture is in the liquid phase. The mass transfer resistance is much lower for the vapor phase than for the liquid phase. Separation factors are often better for vapor separation than for pervaporation.[11–13]

A recent work showed that it was indeed possible to treat the pyrolytic aqueous product by membrane vapor permeation. Cranford[14] developed a hydrophilic membrane from polyetherimide and polyvinyl pyrrolidone. In a pilot test 23% of total feed water was collected on the permeate side, and its purity was higher than 99.97%.

A new process for the treatment of aqueous pyrolysis products is now envisaged. A new membrane will be developed that is preferentially permeable to organic compounds. Then, a module based on hydrophilic water selective membrane and a module based on hydrophobic organic selective membrane are placed in series. A part of the retentate from the latter module is returned to the feedstock. This process would allow the separate recovery of purified water and pyrolytic oil.

The objective of this work was to prepare organic selective membranes and membrane modules based on poly(vinylidene fluoride) (PVDF) material. PVDF material has been used to prepare microfiltration, ultrafiltration, and pervaporation membranes[15–18] and is known to be hydrophobic from its contact angle of 94 to 102°.[19] It is also known to be an elastomeric material with a glass transition temperature of −44°C.[20] The morphology of the membranes so prepared has been investigated, and membranes have been further tested for their performance for vapor separation.

EXPERIMENTAL

Materials

PVDF, Kynar 740™, was purchased from Elf Atochem (Philadelphia). Polyetherimide (PEI), Ultem™, was supplied by General Electric Co. (Pittsfield). *N*-Dimethylformamide (DMF), *N*-dimethylacetamide (DMAC), and *N*-methylpyrrolidone (NMP) were purchased from Aldrich (Milwaukee). Dimethylsulfoxide (DMSO) was from

Table I Hollow-Fiber Spinning Conditions

Membrane	1	2	3	4	5	6	7	8
Composition of spinning solution (wt %)								
PVDF	20	24	24	24	20	20	22	24
Solvent								
DMAC	80	76	76	76				
DMSO					80	80	78	76
Nitrogen pressure, kPa gauge[a]	59	69	69	69	41	41	45	76
Internal coagulant flow rate (g/min)	3.6	1.6	1.6	1.4	9.6	9.6	9.6	9.6
Air gap (cm)	10	11	11	11	10	10	10	10
Polymer solution temperature (°C)	20	22	22	22	40	60	40	40
Internal and external coagulant temperature (°C)	10	23	23	23	23	23	23	23

Membrane	9	10	11	12	13	14	15	16
Composition of spinning solution (wt %)								
PVDF	20	20	20	19.4	24	22	22	28
Solvent								
DMF	80							
NMP		80	61	58.2	49	68	68	62
Additive								
Water			3	3.33	4			
Acetone			16	19.4	23			
Propionic acid						10	10	10
Nitrogen pressure, kPa gauge[b]	38	69	28	45	69	52	31	103
Internal coagulant flow rate (g/min)	2.8	3.2	15	20	11	20	16	25
Air gap (cm)	10	10	30	30	30	30	30	60
Polymer solution temperature (°C)	20	20	20	40	40	23	50	80
Internal coagulant temperature (°C)	10	10	20	40	40	20	50	45
External coagulant temperature (°C)	23	23	20	40	40	20	50	45

[a] Polymer solution flow rate increases with an increase in nitrogen pressure.
[b] Polymer solution flow rate increases with an increase in nitrogen flow rate.

BDH (Toronto). All polymers and solvents were used without further purification.

Hollow-Fiber Spinning

Hollow fibers were spun by the dry–wet spinning method. Two types of spinnerets were used for spinning. One, presented schematically in Figure 1, is furnished with two concentric exits for internal coagulant and polymer solution. The procedure of hollow-fiber spinning was described by Liu et al.[21] The compositions of polymer solutions used for the hollow-fiber spinning and the spinning conditions are summarized in Table I.

Some composite membranes were also prepared in the following way. A polyetherimide hollow fiber (membrane 17) was spun from 20 wt % polymer solution in NMP. Nitrogen pressure, internal coagu-

Table II Conditions of Hollow-Fiber Coating

Membrane	17[a]	18	19	20
Number of coatings	0	1	1	2
Composition of coating solution (wt %)				
PVDF		2	8	8
DMSO		15	15	15
Acetone		83	77	77

[a] Conditions of spinning as given in the text.

lant flow rate, air gap, and temperatures of polymer solution, internal, and external coagulants were 28 kPa gauge, 31 g/min, 14 cm, 20°C, respectively. Then, the internal surface of the hollow fiber was coated with dilute PVDF solutions. The number of coatings and the compositions of the coating solutions are listed in Table II. The polymer solution was pumped to the bore side of hollow fibers for 30 s. Then, the polymer solution in the hollow fiber was removed by applying air pressure on one end of the hollow fiber, leaving a thin layer of PVDF solution at the internal wall of the hollow fiber. The solvent was then evaporated for 10 min under an air flow rate of 5.7 L/min. Further solvent evaporation was achieved under an air stream of 28.3 L/min for 1 h.

Membrane Characterization

The hollow-fiber membranes were characterized by outside diameter, membrane thickness, and membrane density (ρ_m). The membrane density was obtained from the equation

$$\rho_m = \frac{A}{\left(\frac{A}{\rho_p} + \frac{(1-A)}{\rho_{\text{wat}}}\right)(1-B)} \tag{1}$$

where A and B are mass fraction of polymer in the membrane and overall shrinkage. ρ_p and ρ_{wat} are densities of polymer and water, respectively. A was determined by weighing a water-wet membrane, drying overnight at 60°C in a ventilated oven, and weighing the dried membrane.[22] Then, A is calculated by

$$A = \frac{(\text{dry membrane weight})}{(\text{wet membrane weight})} \tag{2}$$

The longitudinal shrinkage of a hollow fiber during drying is determined by measuring the length of the hollow fiber before and after the drying.

$$S_{\text{long}} = \frac{(\text{wet length} - \text{dry length})}{(\text{wet length})} \tag{3}$$

Assuming the shrinkage to the radial direction and in the wall thickness is equal to that in the longitudinal direction. B is calculated by

$$B = 1 - (1 - S_{\text{long}})^3 \tag{4}$$

The void fraction is calculated by

$$\epsilon = \frac{\left(\frac{1}{\rho_m} - \frac{1}{\rho_p}\right)}{\left(\frac{1}{\rho_m}\right)} \tag{5}$$

Table III Characteristics of Hollow Fibers

Membrane	1	2	3	4	5	6	7	8
Outside diameter (mm)	1.40	1.52	1.40	1.29	1.79	1.79	1.90	2.02
Wall thickness (mm)	0.17	0.16	0.26	0.31	0.20	0.20	0.21	0.20
ρ_m (g/cm^3)	0.605	0.692	0.605	0.587	0.340	0.348	0.358	0.360
ϵ	0.656	0.607	0.656	0.670	0.809	0.804	0.799	0.798
Membrane	9	10	11	12	13	14	15	16
Outside diameter (mm)	1.50	1.42	1.67	1.59	1.48	1.80	1.86	1.44
Wall thickness (mm)	0.12	0.36	0.10	0.11	0.10	0.09	0.09	0.15
ρ_m (g/cm^3)	0.730	0.426	0.636	0.569	0.802	0.712	0.592	0.912
ϵ	0.585	0.761	0.640	0.676	0.544	0.595	0.663	0.480

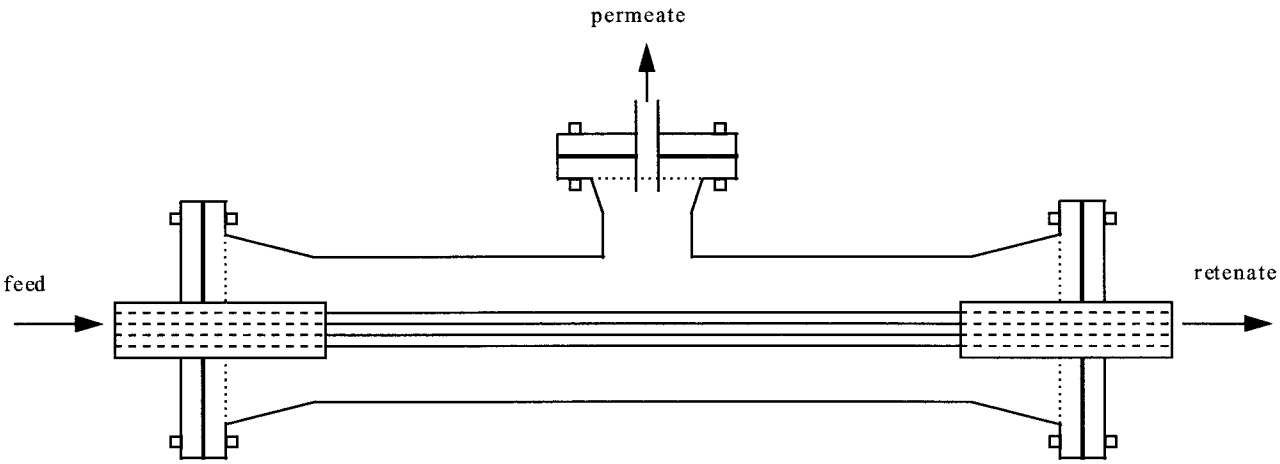

Figure 2 Schematic presentation of a hollow-fiber module.

The membranes were also characterized by scanning electron microscopic (SEM) techniques of the cross section, which were taken by JOEL-JSM-849.

Preparation of Membrane Modules and Hollow-Fiber Testing

A bundle of 10 hollow fibers was made. Both ends of the hollow-fiber bundle were potted in epoxy-glue to tubular molds, the diameter of which was 1.27 cm. The length of the hollow fiber effective for vapor permeation was 30 cm. The design of a hollow-fiber module is illustrated schematically in Figure 2. The hollow-fiber testing equipment is illustrated schematically in Figure 3. The feed was a 50 wt % aqueous solution of 1-propanol. The feed mixture was supplied to the system by a volumetric piston pump and heated for evaporation before entering the bore side of the hol-

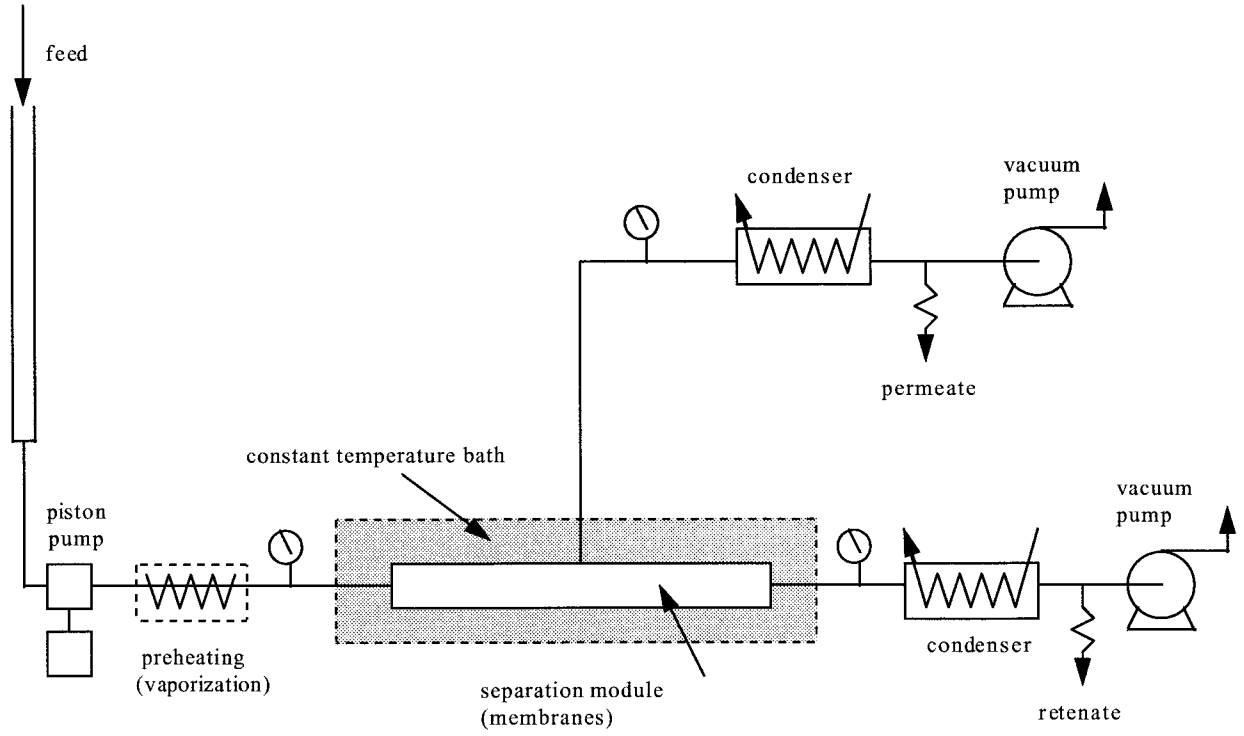

Figure 3 Schematic presentation of a hollow-fiber separation system.

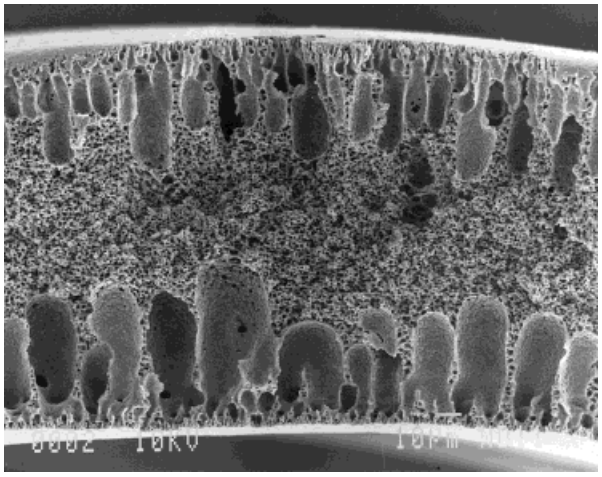

Figure 4 SEM picture of membrane 2.

low-fiber module. Vacuum was applied on both retentate and permeate sides to maintain the transmembrane pressure drop. The retentate side pressure was kept between 28.5 to 57.0 kPa, while the permeate side pressure was kept between 15.0 to 25.0 kPa. Both retentate and permeate were condensed in condensers cooled by ice-cold water, and the flow rates were determined by weighing retentate and permeate samples collected during a predetermined period. The ratio of the permeate flow rate to the retentate flow rate was about 0.5 for each experiment. The analysis of feed, retentate, and permeate samples were done by refractive index measurement.

The performance of hollow fibers was characterized by permeance (P/δ), which was obtained by

$$\left(\frac{P}{\delta}\right)_i = \frac{Q_i}{St(p_{\text{bore}}X_{\text{ave},i} - p_{\text{perm}}X_{\text{perm},i})} \quad (6)$$

where Q_i is mol of ith species collected during a period t (s) through membrane area, S (m^2), in the condenser. p_{bore} and p_{perm} (Pa) are total pressures on the bore (feed and retentate) side and the permeate side of the hollow fiber, respectively. $X_{\text{ave},i}$ is the average of mol fractions of the ith species in the feed and retentate, and X_{perm} is the mol fraction of the ith species on the permeate side, respectively. A similar equation was derived and used to calculate $(P/\delta)_j$. In this work, water and 1-propanol are defined as the ith and jth species. The ideal separation factor (α_j^i) was obtained by

$$\alpha_j^i = \frac{\left(\frac{P}{\delta}\right)_i}{\left(\frac{P}{\delta}\right)_j} \quad (7)$$

RESULTS AND DISCUSSION

Membrane Characterization

Membrane geometry and some characterization parameters of the hollow fibers are listed in Table III. The outside diameters of the hollow fibers were in the range from 1.40 to 2.02 mm. The wall thicknesses were in the range from 0.09 to 0.26 mm. The larger outer diameter did not necessarily

Table IV Hollow-Fiber Performance Data

Membrane	1	2	3	4	5	6	7	8
$(P/\delta)_{\text{pro}} \times 10^7$ (mol m^{-2} s^{-1} Pa^{-1})	2.37	2.99	3.71	0.56	27.5	22.7	15.8	11.7
$(P/\delta)_{\text{wat}} \times 10^7$ (mol m^{-2} s^{-1} Pa^{-1})	13.0	15.4	14.3	6.46	62.0	22.5	67.2	41.4
$\alpha_{\text{pro}}^{\text{wat}}$	5.49	5.15	3.87	11.5	2.25	0.99	4.26	3.55

Membrane	9	10	11	12	13	14	15
$(P/\delta)_{\text{pro}} \times 10^7$ (mol m^{-2} s^{-1} Pa^{-1})	0.146	27.0	1.75	0.139	0.069	1.45	0.604
$(P/\delta)_{\text{wat}} \times 10^7$ (mol m^{-2} s^{-1} Pa^{-1})	5.16	27.0	5.91	1.53	2.77	9.83	7.11
$\alpha_{\text{pro}}^{\text{wat}}$	35.3	1.0	3.38	10.98	40.0	6.76	11.76

Membrane	16	17	18	19	20
$(P/\delta)_{\text{pro}} \times 10^7$ (mol m^{-2} s^{-1} Pa^{-1})	0.0143	0.00817	0.514	1.27	1.15
$(P/\delta)_{\text{wat}} \times 10^7$ (mol m^{-2} s^{-1} Pa^{-1})	1.15	8.313	4.86	4.88	4.99
$\alpha_{\text{pro}}^{\text{wat}}$	83.3	1031	9.43	3.85	4.35

correspond to the larger wall thickness. It is difficult to find any correlation between the condition of membrane preparation and the membrane geometry. The membrane density defined by eq. (1) ranged from 0.340 to 0.912. Correspondingly, void fraction, ϵ, calculated by eq. (5) changed from 0.809 to 0.480. Void fraction is a bulk property of the membrane. Electron microscopic picture shown in Figure 4 indicates that the void is located primarily in the porous sublayer underneath the dense surface layer. The void fraction should have, therefore, no effect on membrane selectivity, which is governed mostly by the dense surface layer. However, a correlation between the void space and the membrane selectivity was observed, as will be shown later.

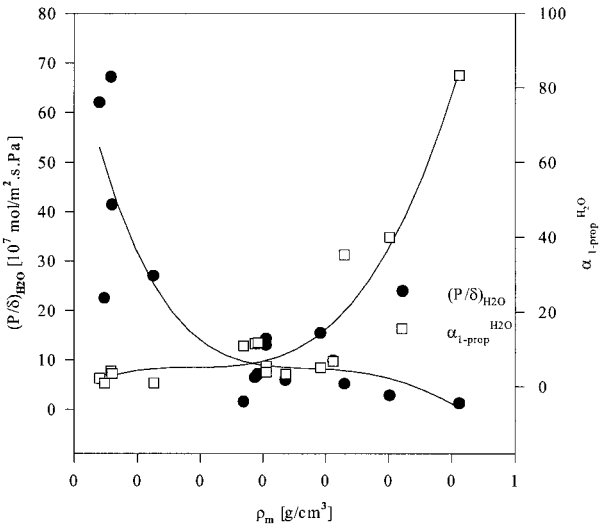

Figure 5 Separation characteristics of PVDF membranes [$(P/\delta)_{wat}$ and α^{wat}_{pro} vs. ρ_m].

SEM Study

The SEM picture taken for hollow fiber 2 (Fig. 4) clearly indicates the presence of thin dense layers both on the internal and external surfaces of the hollow fiber. Large fingerlike voids developed from both ends of the cross section, leaving in the center a spongelike layer. This is natural, as the skin layer and the void are formed by the penetration of the coagulant from both the interior and exterior surfaces of the hollow fiber.

Membrane Performance

All membrane performance data are listed in Table IV. The data indicate that most of PVDF membranes were water selective, which was opposite to our initial intention to prepare organic selective membranes. Comparing hollow-fiber spinning conditions listed in Tables I–II and the membrane performance data listed in Table IV, it is difficult to find any correlation between spinning parameters and the membrane performance. Nevertheless, some general conclusion can be obtained between the membrane density listed in Table III and the membrane performance data listed in Table IV. In Figure 5, $(P/\delta)_{wat}$ and α^{wat}_{pro} are plotted versus ρ_m. Even though the experimental data scatter quite significantly, the presence of strong correlations between these parameters is undeniable. $(P/\delta)_{wat}$ decreases and α^{wat}_{pro} increases with an increase in ρ_m. As previously explained, ρ_m is a bulk quantity related to void fraction of the porous sublayer and should have nothing to do with the property of the dense surface layer that is supposed to govern the membrane performance. The occurrence of a relationship between the membrane permeability and selectivity data and ρ_m, therefore, allows us to draw either one of the following conclusions: (1) the structure of the dense surface layer is related to the structure of the porous sublayer. When the sublayer becomes more porous, the transport path through the dense surface layer becomes wider. (2) The structure of the dense surface layer is not related to that of the porous sublayer. However, the membrane performance is governed not only by the dense surface layer but also by the porous sublayer.

It is also interesting to note that membranes 13 and 16 that have α^{wat}_{pro} values equal to or greater than 40 were spun from polymer solutions containing volatile solvents such as acetone and propionic acid. This suggests the formation of the surface layer with a very narrow transport path when the solvent evaporates quickly during hollow-fiber spinning.

Another interesting observation is that the permeation of 1-propanol through the PEI membrane (membrane 17) was almost completely prevented, resulting in a very high water selectivity. When the PEI membrane was coated with a PVDF layer (membranes 18, 19, and 20), propanol permeation was enhanced greatly while water permeation was slightly reduced, resulting in much lower water selectivities. The results can be explained by a series model of membrane transport. When a highly water selective PEI layer and a far less water selective, or even 1-propanol selective, PVDF layer are connected in series, the overall

performance of the composite membrane is governed by a layer of higher resistance. In this case, the governing layer seems to be the PEI layer, which results in a water selective composite membrane. The more the PVDF concentration in the polymer solution or the more the number of the coating layers, the greater the transport of propanol. The above results indicate the intrinsically hydrophobic nature of PVDF material.

CONCLUSIONS

The following conclusions can be drawn from the experimental results: (1) Asymmetric hollow-fiber membranes can be prepared from PVDF material by the wet–dry spinning method. (2) The membranes so prepared are water selective in the separation of water/1-propanol mixtures despite the hydrophobic nature of PVDF material. (3) The selectivity of the membrane increases and the flux decreases with an increase in the membrane density. (4) Addition of a volatile organic solvent in the spinning solution increases the membrane density, resulting in a higher membrane selectivity. (5) Coating of polyetherimide hollow fibers with a PVDF layer decreases the water selectivity.

REFERENCES

1. C. Roy, B. de Caumia, H. Pakdel, G. Couture, and B. Labrecque, in *6th European Conference on Biomass for Energy, Industry and Environment,* Elsevier, New York, 1992, p. 975.
2. C. Roy, B. de Caumia, D. Blanchette, H. Pakdel, G. Couture, and A. E. Schwerdtfeger, in *Remediation Winter 1994 / 95,* Wiley, New York, 1994, p. 111.
3. H. Pakdel, G. Couture, and C. Roy, *Tappi J.,* **77,** 205 (1994).
4. R. H. Perry and D. Green, *Perry's Chemical Engineer's Handbook,* Vol. 21, McGraw-Hill, New York, 1984, pp. 64–65.
5. M. Soto, J. A. Field, G. Lettinga, R. Méndez, and J. M. Lema, *J. Chem. Technol. Biotechnol.,* **52,** 163 (1991).
6. S. E. Jorgensen, *Industrial Waste Water Management,* Elsevier, Amsterdam, 1979, p. 104.
7. D. Leszczynska and A. L. Kowal, in *Physical Methods for Water and Wastewater Treatment,* Pergamon, Oxford, 1979, p. 123.
8. K. Urano, E. Yamamoto, M. Tonegawa, and K. Fujie, *Water Res.,* **25,** 1459 (1991).
9. J. P. Bechac, P. Boutin, B. Mercier, and P. Nuer, *Traitements des Eaux Usées,* Eyrolles, Paris, 1984, p. 202.
10. R. L. Culp, G. Mack Wesner, and G. L. Culp, *Handbook of Advanced Wastewater Treatment,* Van Nostrand Reinhold Co., New York, 1978, p. 166.
11. K. Okamoto, N. Tanihara, H. Watanabe, H. Kita, A. Nakamura, Y. Kusuki, and K. Nakagawa, *J. Membr. Sci.,* **68,** 53 (1992).
12. B. Will and R. N. Lichtenthaler, *J. Membr. Sci.,* **68,** 119 (1992).
13. B. Will and R. N. Lichtenthaler, *J. Membr. Sci.,* **68,** 127 (1992).
14. R. J. Cranford, Ph.D. Thesis, Department of Chemical Engineering, Université Laval, 1995.
15. R. Field, S. Hang, and T. Arnot, *J. Membr. Sci.,* **86,** 291 (1994).
16. S. Murani, A. Bottino, and G. Capannelli, *J. Membr. Sci.,* **16,** 181 (1983).
17. T. Uragami, M. Fujimoto, and M. Sugihara, *Polymer,* **21,** 1047 (1980).
18. T. Uragami, M. Fujimoto, and M. Sugihara, *Agnew. Makromol. Chem.,* **95,** 45 (1981).
19. Y. Fujii, S. Kigoshi, H. Iwatani, and M. Aoyama, *J. Membr. Sci.,* **72,** 53 (1992).
20. J. Brandrup and E. H. Immergut, *Polymer Handbook,* 3rd ed., Wiley, New York, 1989, p. VII-379.
21. T. Liu, S. Xu, D. Zhang, S. Sourirajan, and T. Matsuura, *Desalination,* **85,** 1 (1991).
22. M. T. So, F. R. Eirich, H. Strathmann, and R. W. Baker, *Polym. Lett. Ed.,* **11,** 201 (1973).